Evaluation of Occupancy Grid Resolution through a Novel Approach for Inverse Sensor Modeling

Roxana Dia, Julien Mottin, Tiana Rakotovao, Diego Puschini, Suzanne Lesecq

Evaluation of Occupancy Grid Resolution through a Novel Approach for Inverse Sensor Modeling

Roxana Dia, Julien Mottin, Tiana Rakotovao, Diego Puschini, Suzanne Lesecq

Univ Grenoble Alpes, CEA, Leti, F-38000 Grenoble, France.
(e-mail: roxana.dia@cea.fr).

Abstract:
Several robotic applications imply motion in complex and dynamic environments. Occupancy Grids model the surrounding environment by a grid composed of a finite number of cells. The probability whether a cell is occupied or empty is computed and updated iteratively based on sensor measurements by considering their uncertainty through probabilistic models. Even if Occupancy Grids have been widely used in the state-of-the-art, the relation between the cell size, the sensor precision and the inverse sensor model is usually neglected. In this paper, we propose a methodology to build the inverse probabilistic model for single-target sensors. The proposed approach is then applied to a LiDAR in order to evaluate the impact of the variation in the sensor precision and the grid resolution on the inverse sensor model. Based on this study, we finally propose a procedure that allows to choose the suitable grid resolution for obtaining a desired maximum occupancy probability in the inverse sensor model.

1. INTRODUCTION

Modern mobile robots evolve in complex *a priori* unknown environments. In these scenarios, the surrounding obstacles are perceived thanks to range sensors such as LiDARs, sonars, radars, Time-of-Flight cameras, vision sensors. However, external conditions, the nature of observed obstacles or even imperfections in the sensor design introduce noise in the measurements. Common approaches translate this uncertainty into a probabilistic distribution called the *Sensor Model* (SM).

The SM gives the likelihood of a specific sensor value knowing a property of the environment such as the distance to the nearest object. Hence, it creates a link between the physical world and the sensor output. The SM can be constructed with analytical approaches taking into account the sensor precision given in its datasheet. Alternatively, it can be experimentally built by analyzing the dispersion of the sensor output subject to a set of predefined physical situations. Sensor Models are consequently often called *generative models* as they can be generated from real situations [Thrun et al. (2005)]. The sensor data interpretation is based on the Bayes' rule applied to the SM: from a *prior* state and with the SM, the Bayes' rule allows to predict the *posterior* state.

These states are defined thanks to the utilization of a model of the surrounding space. An environment model can be seen as a computational representation of the space where the robot is operating [Burgard and Hebert (2008)]. Introduced in the mid-1980s by Moravec and Elfes [Moravec and Elfes (1985)], *Occupancy Grids* (OGs) constitute one of the most popular frameworks for environment model definition. They map a portion of the surrounding space into a partition composed of cells. Each cell of the OG can be either occupied by an obstacle or empty. The objective of the perception task is then to obtain the occupancy probability for each cell taking into account the sensors readings.

The SM gives information on the position of the obstacles rather than the occupancy of a specific region. To deduce occupancy probabilities, OGs rely on a robust mathematical approach presented by Elfes [Elfes (1989)]. It defines a formal methodology that produces an *Inverse Sensor Model* (ISM) from a SM and a specific partition of the space. This ISM relates the sensor measurements to the occupancy probability for all cells. An appealing property of this approach is that it naturally propagates the sensing precision to the occupancy evaluation. Uncertainty captured by the SM is converted into an equivalent uncertainty for the ISM. Consequently, the state of the environment is estimated with the same precision of the sensor.

This theoretical approach relies on the enumeration of all possible grid configurations whose number is exponentially growing with the number of cells. The computation of OGs with a large number of cells becomes therefore intractable in practice. To overcome this limitation, approximations in the ISM generation have been proposed [Konolige (1997); Adarve et al. (2012)]. However, these methods break the link between the generative model and the OG, to offer computationally effective formulations. Moreover, they are tuned for specific sensor and grid configurations and cannot support the study of the influence of grid parameters and sensor precision.

The contributions of this paper are threefold. Firstly, a new methodology for the ISM construction is proposed. It introduces no additional approximation compared to the

original OG formulation. This methodology can be applied to sensors that exhibit a single-target behavior *i.e.* whose output is caused by a unique obstacle, assumed to be the nearest one, such as LiDARs and depth pixels of time-of-flight cameras. For these sensors, the proposed method has a computational cost proportional to the number of cells in the grid. Since the new method naturally fits in the original OG framework proposed in [Elfes (1989)], it also propagates the original precision of the sensor to the ISM. Secondly, by applying our methodology to a LiDAR, we analyze the impact of the grid resolution and the sensor precision on the occupancy estimation. And finally, a novel method that allows to properly choose the grid resolution is proposed. This method allows to achieve a predefined maximum occupancy probability in the ISM taking into account the sensor precision and its output. It is therefore useful when modeling the ISM, because it allows to propagate the variations in the sensor precision and the cells size in the grid to the occupancy evaluation.

This paper is organized as follows. Section 2 introduces background theory, related works and the present contributions. Section 3 details the proposed methodology for the computation of inverse models of single-target sensors. The study of the impact of the grid resolution and of the sensor precision on the ISM is presented in Section 4. Then, the proposed methodology for choosing the appropriate grid resolution is shown in Section 5. Finally, Section 6 concludes the paper.

2. MOTIVATION

2.1 Mathematical background

Ω refers to a continuous $1D$, $2D$ or $3D$ spatial reference. A *grid* $\mathcal{G}$ is a bounded continuous subset of Ω, partitioned into a finite number of N disjoint cells. Let c_i denotes a cell identified by a unique index i, $i \in \{0, \dots, N-1\}$. No additional hypothesis is set on the size of cells and the way the grid is arranged. A physical *obstacle* A is a continuous and bounded subset of Ω. For $i \in \{0, \dots, N-1\}$ c_i is occupied by A if $A \cap c_i \neq \emptyset$, whereas c_i is not occupied by A if $A \cap c_i = \emptyset$. The *state* s_i of cell c_i is the outcome of a binary random experiment. The value of s_i can be any of the two outcomes: $s_i \in \{o_i, e_i\}$, where o_i is the event *"c_i is occupied"* and $e_i = \neg o_i$ is the event *"c_i is empty"*. Since o_i and e_i are complementary events:

$$P(o_i) + P(e_i) = 1 \tag{1}$$

Let z be the sensor output caused by a measure toward an obstacle located at position x, where x has the same dimension as the considered spatial reference Ω. The SM refers to the probability density function $p(z|x)$. It estimates the probability that the sensor response z will be in a given interval, knowing that an obstacle is positioned in x. Thus, this distribution encodes the precision of the sensor [MacKinnon et al. (2006)].

The *occupancy probability* denotes the distribution $P(o_i|z)$ which estimates the probability of the event o_i given the sensor measurement z. The ISM refers to the set of $P(o_i|z)$, $i \in \{0, ..., N-1\}$. The ISM allows to solve the perception problem for a single sensor, giving all occupancy probabilities from a sensor measurement. The occupancy of different cells is assumed to be conditionally independent with respect to z:

$$\forall i \neq j, P(s_i \wedge s_j|z) = P(s_i|z)P(s_j|z) \tag{2}$$

With these definitions, the methodology proposed by Elfes for the computation of the ISM is now shortly introduced. Applying the Bayes' theorem on $P(o_i|z)$, it comes for all $i \in \{0, ..., N-1\}$:

$$P(o_i|z) = \frac{p(z|o_i) \cdot P(o_i)}{p(z)} \tag{3}$$

From the decomposition on the two complementary events o_i and e_i, (3) becomes:

$$P(o_i|z) = \frac{p(z|o_i) \cdot P(o_i)}{p(z|o_i) \cdot P(o_i) + p(z|e_i) \cdot P(e_i)} \tag{4}$$

$P(o_i)$ and $P(e_i)$ evaluate the prior information about the occupancy of cell c_i. If prior information is not available, the non-informative prior hypothesis $P(o_i) = P(e_i) = 1/2$ can be adopted. It comes:

$$P(o_i|z) = \frac{p(z|o_i)}{p(z|o_i) + p(z|e_i)} \tag{5}$$

Equation (5) requires the computation of $p(z|e_i)$ and $p(z|o_i)$. The idea is then to deduce the distribution $p(z|s_i)$ from the SM $p(z|x)$ with $s_i \in \{o_i, e_i\}$. To this purpose, the total probability law is applied over all possible grid configurations as follows:

$$p(z|s_i) = \sum_{G_k^{s_i}} p(z|G_k^{s_i} \wedge s_i) \cdot P(G_k^{s_i}) \tag{6}$$

$G_k^{s_i}$ refers to a grid that has no state information for cell c_i: $G_k^{s_i} = (s_0, \dots, s_{i-1}, s_{i+1}, \dots, s_{N-1})$. Thereby, $G_k^{s_i} \wedge s_i = (s_0, \dots, s_{i-1}, s_i, s_{i+1}, \dots, s_{N-1})$. Hence, $G_k^{s_i} \wedge s_i$ represents the configuration of a grid where the state of cell c_i is set to s_i and the state of the other cells are enforced in $G_k^{s_i}$.

Equations (5) and (6) underline the strong relationship between the occupancy probability and the SM. Moreover, they demonstrate that the occupancy probability is influenced by the partition of the grid, and in particular by the cell size. In (6), $p(z|G_k^{s_i} \wedge s_i)$ can be computed thanks to the SM since the configuration of the grid is known through $G_k^{s_i} \wedge s_i$. However, despite the knowledge of the grid configuration, evaluating $p(z|G_k^{s_i} \wedge s_i)$ for multi-target sensors, *i.e.* whose output may be caused by one or several obstacles, is not trivial since the measurement can be issued from obstacles located on several occupied cells. Furthermore, the number of grid configurations where the state of a single cell is known is 2^{N-1}. Thus, the number of elements in the sum (6) grows exponentially with the number of cells in the grid, preventing practical implementation of this approach.

2.2 Related work

To overcome the implementation burden, several solutions can be found in the literature. For instance, [Elfes (1989)] uses grids with a "reasonable" number of cells. Since in practice (6) is intractable for large grids, many works proposed simplified methods for the construction of the ISM. The first set of solutions consists in providing an analytical form of $p(z|s_i)$ and producing the ISM through (3). In this case, $p(z|s_i)$ is modeled as a function of

the distance to cell c_i from the sensor, with additional parameters that express the sensor uncertainty. Such a model is based on Gaussian distribution in [Konolige (1997)], and on power functions in [Yguel et al. (2006)].

Other authors avoid the calculation of $p(z|s_i)$ by providing an analytical form of the ISM $P(o_i|z)$ as a function of the distance of cell c_i. In [Payeur et al. (1998); Gartshore et al. (2002); Einhorn et al. (2011); Adarve et al. (2012)], the ISM is based on a Gaussian function where the standard deviation is parametrized in order to reflect the sensor uncertainty. Examples of such models applied to stereo pairs can be found in [Li and Ruichek (2013)] and [Nguyen et al. (2012)]. For laser scanners, a linear model is proposed in [Weiss et al. (2007)].

Simpler inverse sensor models return only three possible probabilities, namely, p_{occ} for occupied, p_{emp} for free region and $p_0 = 1/2$ for unknown, where $p_{occ} > p_0 > p_{emp}$ [Thrun et al. (2005); Hornung et al. (2013)].

Finally, more recent works focussed on the direct formulation of the ISM from the SM in order to reduce its computational cost [Kaufman et al. (2016)].

2.3 Paper contribution

Previous works suffer from three limitations. Firstly, by definition, the occupancy denotes the state of a region, and not an obstacle position. To enable the computation of the ISM, previous works provide analytical models for $p(z|s_i)$ or $P(o_i|z)$ as functions of the distance to cell c_i. Their formulation does not take the cell size or shape into account. Hence, they do not allow the study of the influence of the grid resolution on the occupancy estimation. Moreover, these methods suggest that the cell size can be chosen as narrow as possible [Homm et al. (2010)], and that sensor measurement can be challenged at any resolution.

Secondly, previous works do not allow to estimate the occupancy probability from the SM. Some are computationally efficient but they poorly capture variations in the sensor precision [Thrun et al. (2005); Hornung et al. (2013)]. The initial relation between the sensor precision and the occupancy estimation proposed in the OG framework is then broken. It becomes consequently nearly impossible to study the uncertainty propagation, and to quantify the confidence of the resulting environment state estimation. Note that these methods are experimentally tuned to match a known sensor configuration for a predefined grid configuration.

Thirdly, focussing on the direct passage from the SM to the ISM in [Kaufman et al. (2016)] led to a formulation that requires a recursive computation at each sensor reading. In fact, after each measurement, $P(o_i)$ and $P(e_i)$ in (4) take the values that were computed at the previous reading. As a consequence, their formulation has a more complex form than the one proposed in the present paper. In addition, their formulation is based on the fact that each measurement coming from a specific ray in the field of view of the sensor cannot pass through occupied regions. However, this is not the case for all types of sensors, e.g. multi-target sensors such as radars or sonars.

(a) $G_k^{o_i}$ grid with $k^* < i$.

(b) $G_k^{o_i}$ grid with $k^* = i$.

Fig. 1. Enumeration of grids knowing that $s_i = o_i$.

(a) $G_k^{e_i}$ grid with $k^* < i$

(b) $G_k^{e_i}$ grid with $k^* > i$.

Fig. 2. Enumeration of grids knowing that $s_i = e_i$.

The present paper proposes a new efficient method for the computation of (6) that allows to build large OGs. The proposed method applies to single-target sensors and makes no additional approximation or hypothesis. Consequently, it is used to study the influence of the grid resolution and the sensor precision variation on the occupancy estimation. Based on this study, it is shown that the sensor precision captured in the SM imposes a maximum resolution for the grid definition to verify a maximum occupancy probability in the ISM. Thus, a method for choosing the grid resolution that allows to achieve a predefined maximum occupancy probability is proposed.

3. SENSOR MODEL INVERSION

3.1 Single-target grid model

A new methodology for the computation of the ISM of single-target sensors is now proposed. As a consequence, Ω is supposed a $1D$ space. In fact, these sensors might be easier to model with uni-dimensional distributions, and to map the $1D$ model in the two-dimensional or three-dimensional space as in [Rakotovao et al. (2015)].

By the definition of single-target sensors, for a given grid configuration $G_k^{s_i} \wedge s_i$, $i \in \{0, ..., N-1\}, k \in \{1, ..., 2^{N-1}\}$ there exists $k^* \in \{0, ..., N-1\}$ such that c_{k^*} is occupied by an obstacle A_{k^*} at position x_{k^*}, and:

$$p(z|G_k^{s_i} \wedge s_i) = p(z|x_{k^*}) \tag{7}$$

The probability $P(G_k^{s_i})$ is equal to $1/2^{N-1}$, since there exist 2^{N-1} possible configurations. Thus, the sum (6) becomes:

$$p(z|s_i) = \sum_{G_k^{s_i}} \frac{p(z|x_{k^*})}{2^{N-1}} \tag{8}$$

The single-target hypothesis allows to state that the number of possible x_{k^*} values is equal to the number of cells in the grid N. Therefore, among the $2^{N-1} - 1$ left configurations, there might be some configurations which share the same value of x_{k^*} and $p(z|x_{k^*})$ with $G_k^{s_i} \wedge s_i$.

Our approach consists in enumerating the number of configurations which share the same value of $p(z|x_{k^*})$.

These configurations can be grouped together in order to factorize (8).

Suppose $s_i = o_i$. Note k^* the index of the first cell being occupied, which is at the distance x_{k^*}. And then, let us count the number of configurations such that the first obstacle is seen at x_{k^*}, knowing that c_i is occupied. Three cases are then possible:

(1) $k^* < i$: all cells c_j such that $j < k^*$, are empty. The cells c_{k^*} and c_i are occupied. The remaining cells might be in any state. Consequently, there are $k^* + 2$ cells with a known state, which is equivalent to say that there are $N - k^* - 2$ cells whose state can be chosen. Thus, 2^{N-k^*-2} of such grid configurations exist. Figure 1 (a) illustrates this: the white cells are the empty cells, the black cells are occupied and the grey cells are in unknown state;
(2) $k^* = i$: cells c_j such that $j < i$, are empty and the cell c_i is occupied. This leaves $N-i-1$ cells with unknown state, and 2^{N-i-1} of such grid configurations exist. Figure 1 (b) illustrates this case;
(3) $k^* > i$: this configuration is not possible. If $k^* > i$ then the closest object would be seen at distance x_i and not x_{k^*}. Thus, there is no grid configuration satisfying $s_i = o_i$ with closest obstacle at x_{k^*}.

Equation (8) then becomes:

$$p(z|o_i) = \sum_{k=0}^{i-1} 2^{N-k-2} \times \frac{p(z|x_k)}{2^{N-1}} + 2^{N-i-1} \times \frac{p(z|x_i)}{2^{N-1}}$$

$$p(z|o_i) = \sum_{k=0}^{i-1} \frac{p(z|x_k)}{2^{k+1}} + \frac{p(z|x_i)}{2^i} \tag{9}$$

Suppose now that $s_i = e_i$. The first object is still supposed to be seen at the distance x_{k^*}. Again, three cases are possible:

(1) $k^* < i$: all cells c_j such that $j < k^*$, are empty. The cell c_{k^*} is occupied and the cell c_i is empty. The remaining cells are in unknown state, which leaves $N - k^* - 2$ cells whose state is not fixed. More, 2^{N-k^*-2} of such grids exist. Figure 2 (a) illustrates this case;
(2) $k^* = i$: is an impossible configuration. The cell at index i cannot be simultaneously empty and occupied;
(3) $k^* > i$: cells $c_j, j < k^*$ are empty and cell c_{k^*} is occupied. The remaining cells are in unknown state, which leaves $N - k^* - 1$ cells whose state is not fixed. 2^{N-k^*-1} of such grids exist. Figure 2 (b) illustrates this case.

As a consequence, equation (8) becomes:

$$p(z|e_i) = \sum_{k=0}^{i-1} 2^{N-k-2} \times \frac{p(z|x_k)}{2^{N-1}} + \sum_{k=i+1}^{N-1} 2^{N-k-1} \times \frac{p(z|x_k)}{2^{N-1}}$$

$$p(z|e_i) = \sum_{k=0}^{i-1} \frac{p(z|x_k)}{2^{k+1}} + \sum_{k=i+1}^{N-1} \frac{p(z|x_k)}{2^k} \tag{10}$$

Finally, summing (9) and (10) leads to:

$$p(z|o_i) + p(z|e_i) = \sum_{k=0}^{N-1} \frac{p(z|x_k)}{2^k} \tag{11}$$

3.2 Single-target inverse sensor model

The ISM of a single-target sensor can now be constructed. Combining (9), (10) and (11) with (5) gives:

$$P(o_i|z) = \frac{\sum_{k=0}^{i-1} \frac{p(z|x_k)}{2^{k+1}} + \frac{p(z|x_i)}{2^i}}{\sum_{k=0}^{N-1} \frac{p(z|x_k)}{2^k}} \tag{12}$$

Using formula (12) it is now possible to evaluate the ISM thanks the computation of a sum with N terms. Recall that the complexity of the classical formulation is $O(2^N)$, while the complexity of the proposed one is linear with respect to the size of the grid.

The single-target inverse sensor formula presented in (12) gives a computationally effective way for OG construction. The uncertainty captured in the SM $p(z|x)$ is translated into occupancy probability with no additional modeling or parameter. Equation (12) links the spatial partition of the grid with the ISM. Moreover, no additional hypothesis has been made on the SM. Complex space-dependent sensor models or even numerical experimental distribution might be used as well, allowing to address a large variety of sensor models.

4. IMPACT OF THE GRID RESOLUTION AND OF THE SENSOR PRECISION ON THE OCCUPANCY ESTIMATION

The proposed formulation is now used in order to show the impact of the grid resolution and of the sensor precision on the occupancy estimation.

Consider first a $1D$ sensor with a constant uncertainty, modeled using a Gaussian distribution with a constant standard deviation σ. Such a model is defined by the following probability density function:

$$p(z|d) = \frac{1}{\sigma\sqrt{2\pi}} e^{-\frac{(z-d)^2}{2\sigma^2}} \tag{13}$$

Here, the sensor measurement z is supposed to be expressed in the same unit as distance d. This assumption holds for instance, for common commercial range sensors such as the RPLiDAR scanner [URL (2015)] which provides drivers to acquire and parse raw sensor outputs.

For this sensor, the manufacturer states that the worst case distance resolution is equal to $1.2\,cm$ in indoor conditions. For the Gaussian distribution (13) it is known that there is a 99% probability that z is in the interval $[d - 3\sigma, d + 3\sigma]$ when the nearest obstacle is at distance d. This allows to choose σ such that $6\sigma = 1.2\,cm$, yielding $\sigma = 0.2\,cm$.

The influence of the grid resolution is now evaluated considering a uniform 1D grid of length $0.5\,m$ with different cell sizes s.

Suppose the sensor senses an obstacle at $z = 25\,cm$. Figure 3 presents the occupancy probability $P(o_i|z = 25)$, $\forall i \in \{0, ..., N-1\}$ for grids with different cell sizes. Depending on the value of s, this sensor measurement leads to totally different occupancy probabilities. Intuitively, this

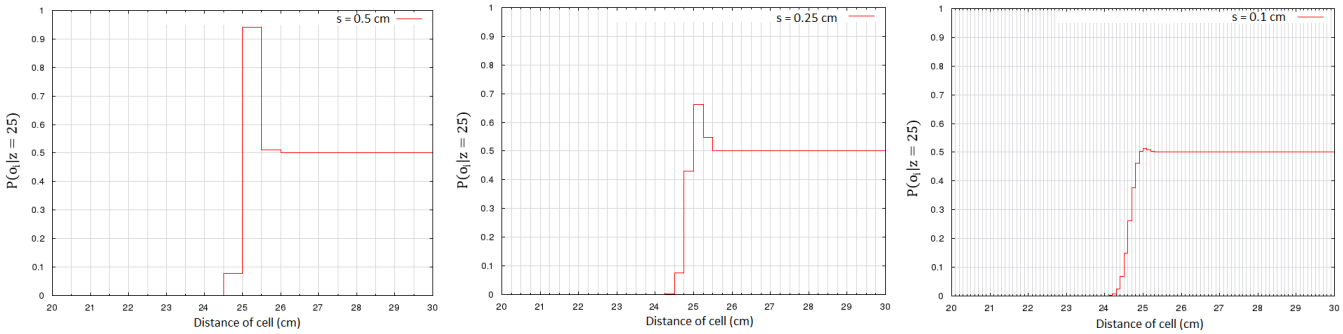

(a) Cell size 0.5 cm. (b) Cell size 0.25 cm. (c) Cell size 0.1 cm.

Fig. 3. Influence of the grid resolution on the ISM for $s_1 = 0.5\ cm$ (a), $s_2 = 0.25\ cm$ (b) and $s_3 = 0.1\ cm$ (c). The sensor has a constant precision $\sigma = 0.2\ cm$ and senses an obstacle at distance $z = 25\ cm$.

can be interpreted in the following way. When the OG challenges the SM at a high resolution, it is hard to derive a strong opinion, whereas it is more easy to express strong opinions on coarse grids. It clearly demonstrates the effect of the grid resolution on the ISM.

On the other side, the impact of the sensor precision σ on the ISM is studied. The same grid of 0.5 m, is used and the obstacle is fixed at $z = 25\ cm$. Three values of σ are tested, namely: $\sigma_1 = 0.1\ cm$, $\sigma_2 = 0.2\ cm$ and $\sigma_3 = 0.3\ cm$, with different cell sizes in each case. The results are presented in table 1. The used cell size and the maximum occupancy probability in the ISM associated to σ_l, $l \in \{1, 2, 3\}$, are respectively presented in columns s_l and P_l. The ratio of each cell size in column s_l over the associated sensor precision σ_l is presented in the first column. Notice that if one uses for two sensor precisions σ_j and σ_k, $j, k \in \{1, 2, 3\}$, an adequate cell size s_j and s_j respectively, verifying $\frac{s_j}{\sigma_j} = \frac{s_k}{\sigma_k}$, then the maximum occupancy probability remains almost the same $P_j \simeq P_k$. This means that for a given probability P_{max}, an output z and a standard deviation σ, there must be a relation that gives the adequate cell size s to use in the grid to get a maximum probability of occupancy P_{max} in the ISM. This relation is shown in the next section.

Table 1. Influence of the grid resolution and different sensor precisions on the ISM.

s_l/σ_l	$s_1\ (cm)$	P_1	$s_2\ (cm)$	P_2	$s_3\ (cm)$	P_3
0.2	0.02	0.5	0.04	0.5	0.06	0.5
0.3	0.03	0.5	0.06	0.5	0.09	0.5
0.5	0.05	0.51	0.1	0.51	0.15	0.51
0.625	0.0625	0.53	0.125	0.53	0.18	0.53
0.8	0.08	0.56	0.16	0.56	0.24	0.56
1	0.1	0.6	0.2	0.6	0.3	0.6
1.25	0.125	0.66	0.25	0.66	0.37	0.66
1.5	0.15	0.72	0.3	0.73	0.45	0.72
2	0.2	0.85	0.4	0.84	0.6	0.84
2.5	0.25	0.94	0.5	0.94	0.75	0.94
3	0.3	0.98	0.6	0.98	0.9	0.98
3.4	0.34	1	0.67	1	1	0.99
3.8	0.38	1	0.75	1	1.13	1
4.2	0.42	1	0.83	1	1.25	1
5	0.5	1	1	1	1.47	1
6	0.6	1	1.19	1	1.78	1

5. CHOICE OF THE APPROPRIATE GRID RESOLUTION

As mentioned above, many studies tend to model the ISM without taking into consideration the influence of the grid resolution and the sensor precision. In this section, a procedure for computing the numerical maximum resolution that overcomes this drawback is proposed.

Consider a sensor output z, a constant standard deviation σ, and a Gaussian SM defined as in (13), then the maximum occupancy probability P_{max} in the 1D grid takes place in cell c_m with:

$$m = \begin{cases} E(\frac{z}{s}) & \text{if } z - x_m < x_{m+1} - z \\ E(\frac{z}{s}) + 1 & \text{otherwise} \end{cases} \tag{14}$$

where $E(.)$ denotes the floor function, and s is a fixed cell size.

In fact, from (12) and by denoting the denominator A, for $i \in \{0, ..., N-2\}$, it comes:

$$\begin{aligned} P(o_{i+1}|z) - P(o_i|z) &= \frac{1}{A}[\frac{p(z|x_{i+1})}{2^{i+1}} - \frac{p(z|x_i)}{2^{i+1}}] \\ &= \frac{1}{2^{i+1}A\sigma\sqrt{2\pi}}[e^{-\frac{(z-is-s)^2}{2\sigma^2}} - e^{-\frac{(z-is)^2}{2\sigma^2}}] \end{aligned} \tag{15}$$

It can be noticed that $\forall i < E(\frac{z}{s})$, $P(o_{i+1}|z) - P(o_i|z) > 0$, and $\forall i \geq E(\frac{z}{s}) + 1$, $P(o_{i+1}|z) - P(o_i|z) < 0$. This implies that P_{max} is equal to $P(o_{m_1}|z)$ or to $P(o_{m_2}|z)$, with $m_1 = E(\frac{z}{s})$ and $m_2 = E(\frac{z}{s}) + 1$.

However, it is clear that if $z - x_{m_1} < x_{m_2} - z$, then $P(o_{m_1}|z) > P(o_{m_2}|z)$, and $P(o_{m_2}|z) \geq P(o_{m_1}|z)$ otherwise. Thus, we conclude that $P_{max} = P(o_m|z)$ for m defined as in (14).

The maximum occupancy probability evaluated from a sensor measurement can now be correlated to the cell size. In fact, once the desired maximum occupancy probability P_{max} is choosen, one can automatically compute the minimum compatible cell size for a given standard deviation σ and a sensor output z. $P(o_m|z)$ is just computed for m defined as in (14) and for different values of s in a given

test set, using formula (12). Then, the smaller cell size that gives P_{max} is selected.

Notice that the maximum occupancy probability not only depends on the grid resolution and the sensor precision but also on its output z.

Generalization

The application of the previous method is not restricted to sensors that possess a Gaussian SM. It can be generalized to a wider type of sensors that have a SM represented in the following theorem where the choice of m is also covered. Once m is chosen, the rest of the previous procedure remains the same.

Theorem 1. For a distance $d \in \mathbb{R}^+$, consider a SM represented by $p(z|d)$ that is:

- Increasing for $z < d$. (P_1)
- Decreasing for $z \geq d$. (P_2)
- For $c \in \mathbb{R}^+$, $p(z|d) = p(z+c|d+c)$. (P_3)

In this case, for a fixed cell size s and a given sensor measurement z, the maximum occupancy probability takes place in cell c_m where:

$$m = \begin{cases} E(\frac{z}{s}) & \text{if } p(z|x_m) > p(z|x_{m+1}) \\ \\ E(\frac{z}{s}) + 1 & \text{otherwise} \end{cases} \tag{16}$$

with $x_k = k.s$, for $k \in \{0, ..., N-1\}$.

Proof.

For $i \in \{0, ..., N-2\}$, (15) is valid:

$$P(o_{i+1}|z) - P(o_i|z) = \frac{1}{2^{i+1}A}[p(z|x_{i+1}) - p(z|x_i)]$$

Using (P_3) for $c = s$ yields to:

$$P(o_{i+1}|z) - P(o_i|z) = \frac{1}{2^{i+1}A}[p(z|x_{i+1}) - p(z+s|x_i+s)]$$

But $x_i + s = x_{i+1}$, then

$$P(o_{i+1}|z) - P(o_i|z) = \frac{1}{2^{i+1}A}[p(z|x_{i+1}) - p(z+s|x_{i+1})]$$

- If $i < E(\frac{z}{s})$, then

$$x_{i+1} \leq sE(\frac{z}{s}) \leq z$$

  Using (P_2), $p(z|x_{i+1}) - p(z+s|x_{i+1}) \geq 0$ and therefore $P(o_{i+1}|z) - P(o_i|z) \geq 0$ in this case.

- If $i \geq E(\frac{z}{s})+1$, a similar reasoning is applied to prove that:

$$z < x_i < x_{i+1}$$

  And then, using (P_1), $P(o_{i+1}|z) - P(o_i|z) \leq 0$.

Thus, the maximum occupancy probability is wether in cell c_{m_1} or in cell c_{m_2} for $m_1 = E(\frac{z}{s})$ and $m_2 = E(\frac{z}{s}) + 1$.

But,

$$P(o_{m_2}|z) - P(o_{m_1}|z) = \frac{1}{2^{m_2}A}[p(z|x_{m_1}) - p(z|x_{m_2})]$$

We can say, finally, that the maximum occupancy probability takes place in cell c_m for m choosen as in (16). ■

6. CONCLUSION

In this paper, a new methodology for the computation of the inverse sensor model for single-target sensors is proposed. Our method is consistent with the occupancy grid framework and allows to estimate the occupancy probabilities with a computational cost proportional to the grid size.

Moreover, this paper demonstrates the strong influence of the grid resolution and the sensor precision on the occupancy estimation. A new procedure allowing to properly choose the grid resolution is also proposed.

Since autonomous mobile robots require to use a wide type of sensors, including multi-target sensors, additional work remains to be done in this regard. We look forward to extend our study in the future and encounter the treated topics in the case of multi-target sensors.

ACKNOWLEDGMENTS

This work has been partly funded by the EUREKA CATRENE TRACE project nb CAT311 under GA nb 152930264 and by the H2020 INSPEX project under GA nb 730953. INSPEX is supported in part by the Swiss Secretariat for Education, Research and Innovation (SERI) under Grant 16.0136 730953. We thank them for their support.

REFERENCES

(2015). RPLIDAR 360 degree Laser Scanner Development Kit. `www.slamtec.com/en-US/rplidar/index`.

Adarve, J.D., Perrollaz, M., Makris, A., and Laugier, C. (2012). Computing Occupancy Grids from Multiple Sensors using Linear Opinion Pools. In *IEEE ICRA*.

Burgard, W. and Hebert, M. (2008). World modeling. In B. Siciliano and O. Khatib (eds.), *Springer Handbook of Robotics*, 853–869.

Einhorn, E., Schroter, C., and Gross, H. (2011). Finding the adequate resolution for grid mapping - cell sizes locally adapting on-the-fly. In *Robotics and Automation (ICRA), 2011 IEEE Int. Conf. on.*

Elfes, A. (1989). *Occupancy Grids: A Probabilistic Framework for Robot Perception and Navigation.* Ph.D. thesis, Carnegie Mellon University, Pittsburgh, PA, USA.

Gartshore, R., Aguado, A., and Galambos, C. (2002). Incremental map building using an occupancy grid for an autonomous monocular robot. *Proceedings of the 7th International Conference on Control, Automation, Robotics and Vision, ICARCV 2002*, 613–618.

Homm, F., Kaempchen, N., Ota, J., and Burschka, D. (2010). Efficient occupancy grid computation on the gpu with lidar and radar for road boundary detection. In *Intelligent Vehicles Symposium.*

Hornung, A., Wurm, K., Bennewitz, M., Stachniss, C., and Burgard, W. (2013). Octomap: an efficient probabilistic 3d mapping framework based on octrees. *Autonomous Robots*, 34(3), 189–206.

Kaufman, E., Lee, T., Ai, Z., and Moskowitz, I.S. (2016). Bayesian occupancy grid mapping via an exact inverse sensor model. In *American Control Conference (ACC), 2016*, 5709–5715. American Automatic Control Council (AACC).

Konolige, K. (1997). Improved occupancy grids for map building. *Autonomous Robots*, 4(4), 351–367.

Li, Y. and Ruichek, Y. (2013). Building variable resolution occupancy grid map from stereoscopic system - a quadtree based approach. In *IEEE Intelligent Vehicles Symposium, Proceedings*, 744–749. doi: 10.1109/IVS.2013.6629556.

MacKinnon, D., Aitken, V., and Blais, F. (2006). A Comparison of Precision and Accuracy in Triangulation Laser Range Scanners. In *Canadian Conf. on Electrical and Computer Engineering*. doi: 10.1109/CCECE.2006.277607.

Moravec, H. and Elfes, A. (1985). High resolution maps from wide angle sonar. In *Proceedings. IEEE ICRA*, volume 2, 116–121.

Nguyen, T.N., Michaelis, B., Al-Hamadi, A., Tornow, M., and Meinecke, M.M. (2012). Stereo-camera-based urban environment perception using occupancy grid and object tracking. *IEEE Transactions on Intelligent Transportation Systems*, 13(1), 154–165.

Payeur, P., Laurendeau, D., and Gosselin, C. (1998). Range data merging for probabilistic octree modeling of 3d workspaces. In *Robotics and Automation, 1998. Proceedings. 1998 IEEE International Conference on*, volume 4, 3071–3078 vol.4.

Rakotovao, T., Mottin, J., Puschini, D., and Laugier, C. (2015). Real-time power-efficient integration of multi-sensor occupancy grid on many-core. In *The 2015 IEEE International Workshop on Advanced Robotics and its Social Impacts*.

Thrun, S., Burgard, W., and Fox, D. (2005). *Probabilistic Robotics (Intelligent Robotics and Autonomous Agents)*. The MIT Press.

Weiss, T. et al. (2007). Robust driving path detection in urban and highway scenarios using a laser scanner and online occupancy grids. In *Intelligent Vehicles Symposium, 2007 IEEE*.

Yguel, M., Aycard, O., and Laugier, C. (2006). Efficient gpu-based construction of occupancy girds using several laser range-finders. In *Intelligent Robots and Systems, 2006 IEEE/RSJ International Conference on*, 105–110. doi:10.1109/IROS.2006.281817.